Supporting information

High-Entropy Conductive Manganese-Based Prussian Blue Analogues Cathode for High-Performance Ammonium-Ion Storage

Zining Li, Liubing Dong *

College of Chemistry and Materials Science, Jinan University

* Corresponding author: donglb@jnu.edu.cn

2. Supporting images and tables

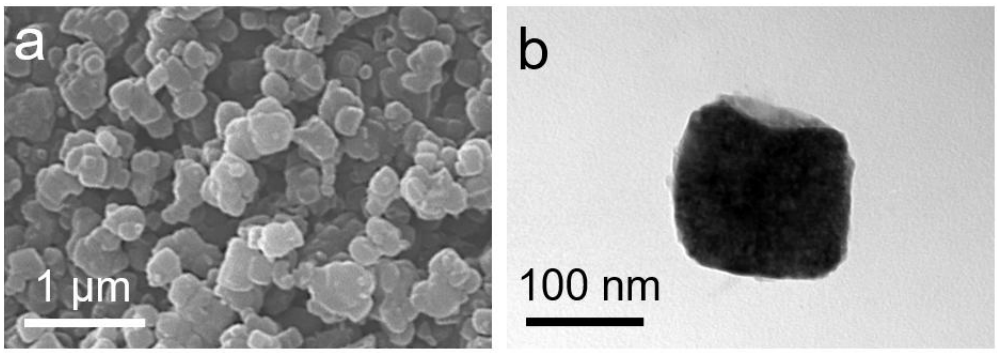

Figure S1. (a)SEM image and (b) TEM image of HEPBA samples (the number of TEM images recorded for each sample exceeded three).

Figure S2. Water contact angle measurements for (a) the MnPBA, (b) HEPBA and (c) HEPBA/CNT cathodes (the contact angle tests were repeated three times).

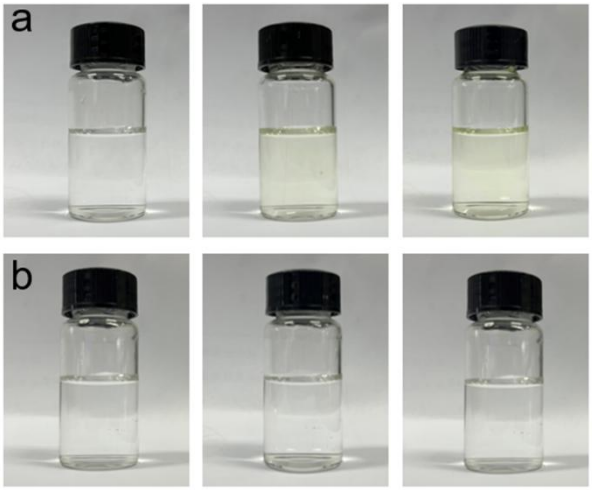

Figure S3. Photographs of the electrolytes in the 3-electrode systems with (a) the MnPBA and (b) the HEPBA/CNT cathodes before cycling (left), after the 1st cycle (middle), and after 50th cycles (right) (the experiments were repeated three times).

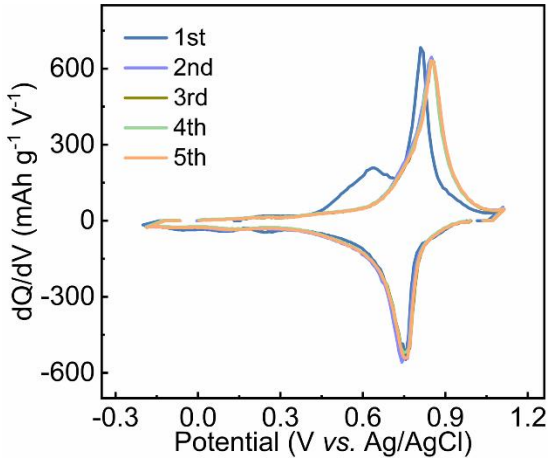

Figure S4. The dQ/dV profiles and of the HEPBA/CNT at 0.1 A/g. The data were verified by at least three repeated tests with high reproducibility.

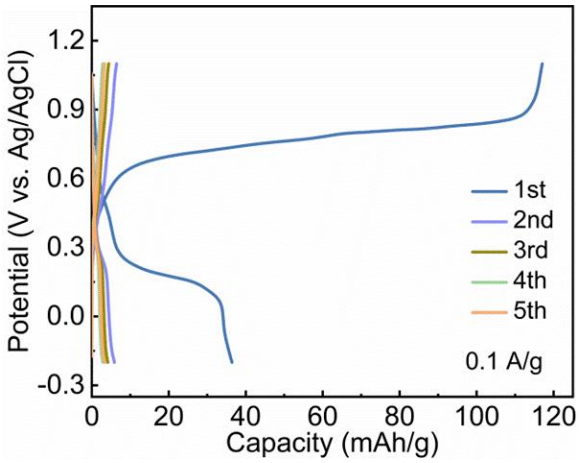

Figure S5. GCD profiles at 0.1 A/g of the MnPBA cathode. The data were verified by at least three repeated tests with high reproducibility.

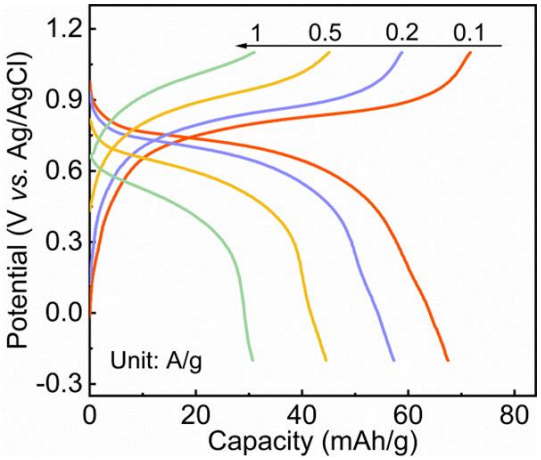

Figure S6. GCD profiles of the HEPBA cathodes. The data were verified by at least three repeated tests with high reproducibility.

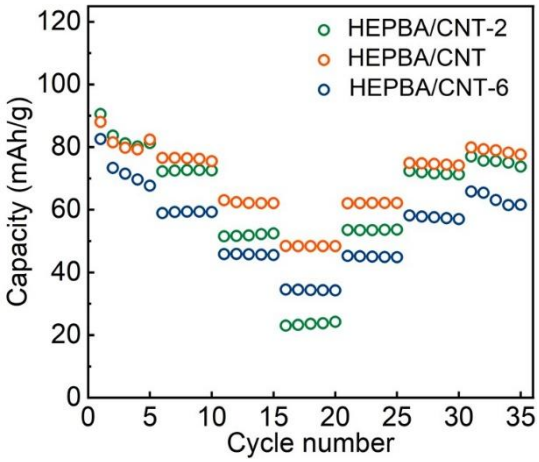

Figure S7. The rate performance of the HEPBA/CNT composite cathodes with different CNT contents. The CNT content in the HEPBA/CNT-2, HEPBA/CNT and HEPBA/CNT-6 samples is 2%, 4% and 6%, respectively. The data were verified by at least three repeated tests with high reproducibility.

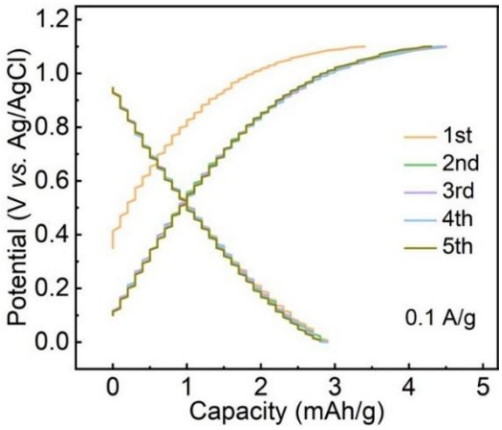

Figure S8. GCD profiles at 0.1 A/g of the CNT cathode in 1 M $(NH_4)_2SO_4$ aqueous electrolyte. The ammonium-ion storage capacity of the CNT cathode is smaller than 3 mAh/g, which means that the CNT component in the HEPBA/CNT composite cathode almost does not contribute capacity. The data were verified by at least three repeated tests with high reproducibility.

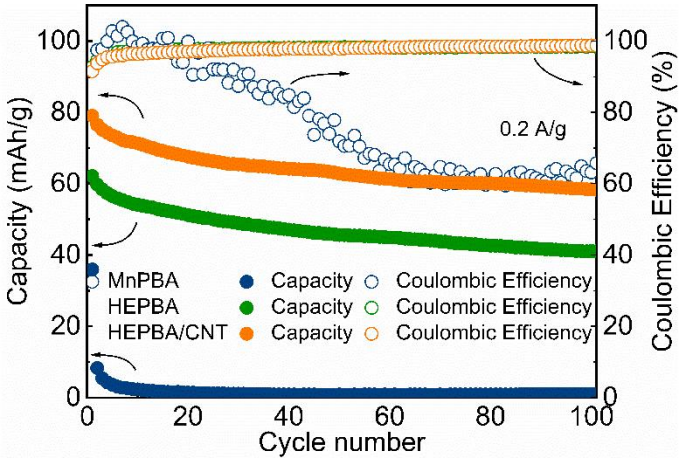

Figure S9. Cycling tests at 0.2 A/g of the MnPBA, HEPBA and HEPBA/CNT cathodes. The data were verified by at least three repeated tests with high reproducibility.

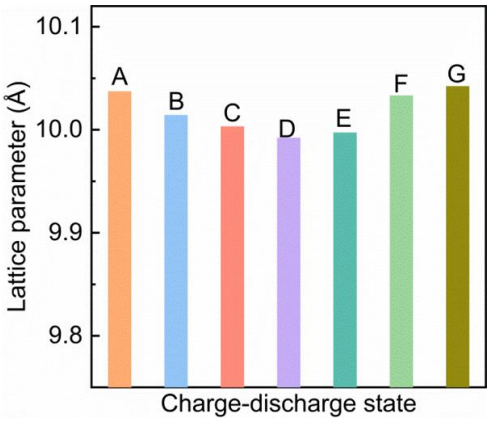

Figure S10. The lattice parameters changes of the HEPBA/CNT cathode during charging-discharging processes. The reversible contraction and expansion indicate the crystal lattice structure is highly stable and exhibits excellent reversibility.

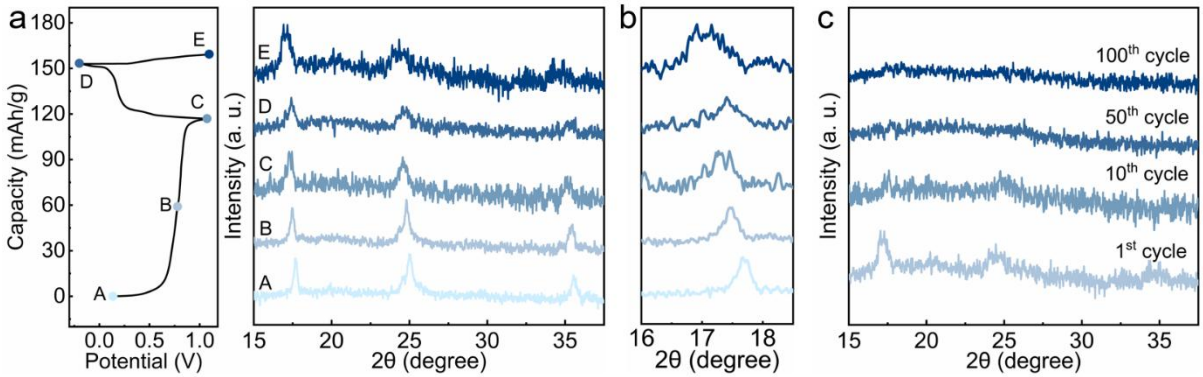

Figure S11. (a) XRD patterns of the MnPBA cathode at different states during the initial charge-discharge process, and (b) the corresponding enlarged XRD patterns. (c) XRD patterns of the MnPBA cathode after different cycles.

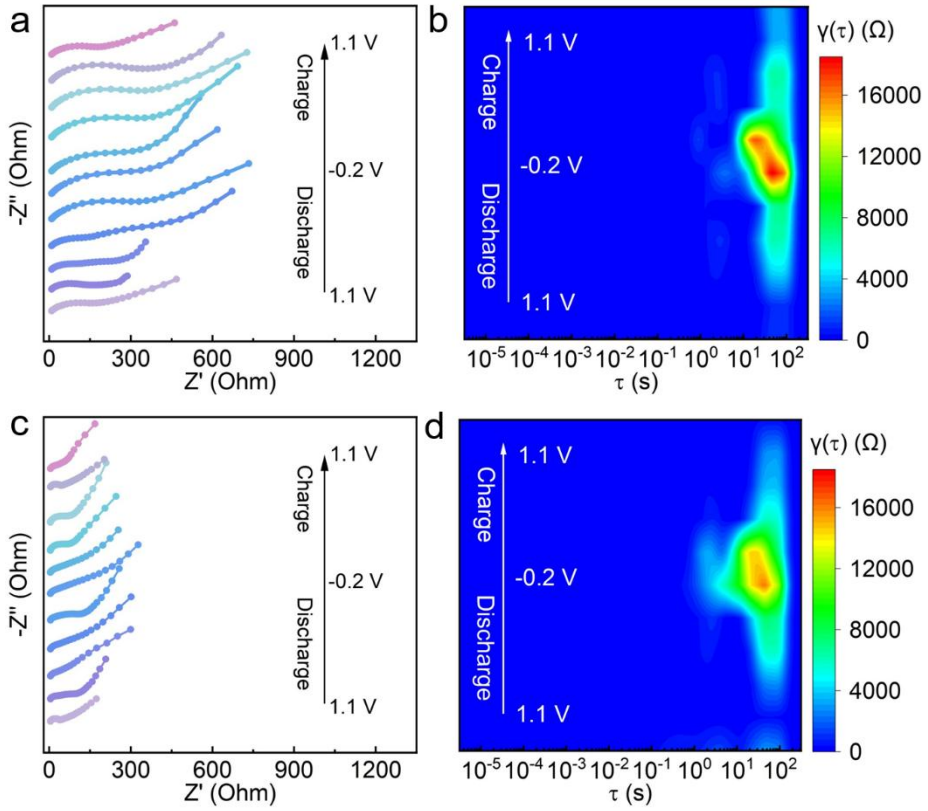

Figure S12. (a) *In-situ* EIS spectra and corresponding (b) DRT diagram of the MnPBA cathode. (c) *In-situ* EIS spectra and corresponding (d) DRT diagram of the HEPBA cathode (the data were verified by at least three repeated tests with high reproducibility). During the charge-discharge process, the MnPBA cathode exhibits pronounced increases in both charge-transfer resistance and ion-diffusion-related resistance, and these resistances fail to recover after charging. Such irreversible changes indicate interfacial degradation and structural instability, which are responsible for the poor ammonium-ion storage performance and inferior cycling stability of the MnPBA cathode. In contrast, the HEPBA cathode shows slight and reversible variations in the EIS spectra. The DRT analysis further displays that the peaks representing contact resistance and charge-transfer resistance remain nearly unchanged, while the ion-diffusion-related resistance increases slightly during the discharge process but returns to the initial level upon the charge process. These results demonstrate that high-entropy structure helps stabilize the structure to suppress interfacial deterioration, thereby ensuring optimized ammonium-ion storage performance.

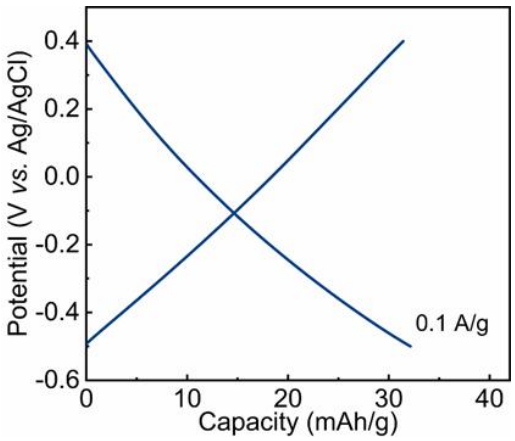

Figure S13. GCD profile of the activated carbon (AC) anode in 1 M $(NH_4)_2SO_4$ aqueous electrolyte. The electrochemical tests were repeated three times.

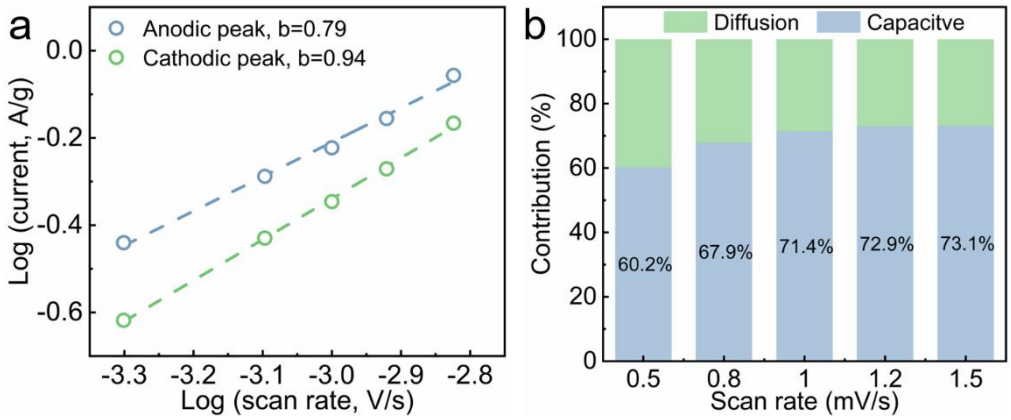

Figure S14. Electrochemical performance of the HEPBA/CNT//AC ammonium-ion hybrid capacitor: (a) The relationship plots between peak current and scan rate; (b) capacitive contributions. The electrochemical tests were repeated three times.

Table S1. Inductively coupled plasma-optical emission spectroscopy and configurational entropy calculation for HEPBA/CNT sample.

	K (wt%)	Mn (wt%)	Fe (wt%)	Co (wt%)	Ni (wt%)	Cu (wt%)	$\triangle S_{conf}$
HEPBA/CNT	19.37±0.05	3.52±0.02	15.54±0.08	3.63±0.01	3.66±0.02	3.94±0.02	1.52R

Note: Data are presented as mean ± standard deviation of three independent measurements.

Table S2. Evolution of K^+ concentration in the electrolyte during the first cycle.

	Charge state	Discharge state
K^+ (mg/L)	6.75 ± 0.09	6.59 ± 0.09

Note: Data are presented as mean ± standard deviation of three independent measurements.

Table S3. Comparison of the ammonium-ion storage performance of the HEPBA/CNT cathode and the literature-reported Prussian blue analogues.

Cathode	**Electrolyte**	**Discharge plateau (V *vs.* Ag/AgCl)**	**Capacity (mAh/g)**	***Ref.***
HEPBA/CNT	1 M $(NH_4)_2SO_4$	0.78	88 (0.1 A/g)	This work
$(NH_4)_{1.47}Ni[Fe(CN)_6]_{0.88}$	1 M $(NH_4)_2SO_4$	0.65	62.6 (0.15 A/g)	[S1]
Na-FeHCF	1 M $(NH_4)_2SO_4$	0.28	61.2 (0.25 A/g)	[S2]
N-CuHCF	2.0 M NH_4NO_3 + 0.01 M $Cu(NO_3)_2$	0.83	60.3 (0.1 A/g)	[S3]
$Ni_2Fe(CN)_6$-R	2 M NH_4Cl	0.55	60.8 (0.06 A/g)	[S4]
NFC	1.0 M NH_4NO_3	0.52	59.1 (0.03 A/g)	[S5]
MnHCF	1 M NH_4TFSI in TEGDME	0.58	104 (0.1 A/g)	[S6]
$Fe_4[Fe(CN)_6]_3$	Saturated $(NH_4)_2SO_4$	0.28	61.4 (0.06 A/g)	[S7]
$Cu_{0.4}Ni_{1.6}Fe(CN)_6$	1 M $(NH_4)_2SO_4$	0.75	52.4 (0.018 A/g)	[S8]
N-CuHCF	5.8 M $(NH_4)_2SO_4$	0.84	47.5 (0.06 A/g)	[S9]
N-CuHCF	1 M $(NH_4)_2SO_4$	0.79	37 (0.06 A/g)	

Mn-PBA@ppy	2.0 M NH_4Otf	0.81	72 (0.1 A/g)	[S10]

Note that HEPBA/CNT cathode delivers a high discharge plateau and capacity in 1 M $(NH_4)_2SO_4$ electrolyte, whereas many other Prussian blue analogues require concentrated or modified electrolytes to achieve comparable performance.

References

[S1] X. Wu, Y. Qi, J. Hong, Z. Li, A. Hernandez and X. Ji, Rocking-chair ammonium-ion battery: a highly reversible aqueous energy storage system, *Angew. Chem. Int. Edit*., 2017, **56**, 13026.

[S2] C. Li, W. Yan, S. Liang, P. Wang, J. Wang, L. Fu, Y. Zhu, Y. Chen, Y. Wu and W. Huang, Achieving a high-performance prussian blue analogue cathode with an ultra-stable redox reaction for ammonium ion storage, *Nanoscale Horiz.*, 2019, **4**, 991.

[S3] X. Zhang, M. Xia, T. Liu, N. Peng, H. Yu, R. Zheng, L. Zhang, M. Shui and J. Shu. Copper hexacyanoferrate as ultra-high rate host for aqueous ammonium-ion storage, *Chem. Eng. J.*, 2021, **421**, 127767.

[S4] H. Yu, J. Xu, C. Deng, M. Xia, X. Zhang, J. Shu and Z. Wang, The nature of the ultrahigh initial coulombic efficiency of $Ni_2Fe(CN)_6$ in aqueous ammonium-ion batteries, *ACS Appl. Energy Mater.*, 2021, **4**, 9594.

[S5] H. Yu, L. Fan, H. Yan, C. Deng, L. Yan, J. Shu and Z. Wang, Optimizing NH_4^+ storage capability of nickel ferrocyanide by regulating coordination anion in aqueous electrolytes, *ChemElectroChem*, 2022, **9**, e202200492.

[S6] H. Zhang, Y. Tian, W. Wang, Z. Jian and W. Chen, Organic ammonium-ion battery: a new strategy for a nonmetallic ion energy storage system, *Angew. Chem. Int. Edit.*, 2022, **61**, e202204351.

[S7] M. Xia, X. Zhang, H. Yu, Z. Yang, S. Chen, L. Zhang, M. Shui, Y. Xie and J. Shu, Hydrogen bond chemistry in $Fe_4[Fe(CN)_6]_3$ host for aqueous NH_4^+ batteries, *Chem. Eng. J.*, 2021, **421**, 127759.

[S8] L. Fan, G. Shu, Y. Liu, H. Yu, L. Yan, L. Zhang and J. Shu, Cu-substituted nickel hexacyanoferrate with tunable reaction potentials for superior ammonium ion storage, *J. Mater. Sci. Technol.*, 2024, **169**, 19.

[S9] J. Han, M. Zarrabeitia, A. Mariani, M. Kuenzel, A. Mullaliu, A. Varzi and S. Passerini, Concentrated electrolytes enabling stable aqueous ammonium-ion batteries, *Adv. Mater.*,

2022, **34**, 2201877.

[S10] Q. Liu, D. Zhang, Y. Yang, Y. Gu, Z. Liang, W. Chen, Y. Wu and L. Hu, Encapsulation of prussian blue analogues with conductive polymers for high-performance ammonium-ion storage, *Adv. Energy Mater.*, 2025, **15**, 2402863.